Record of paleofluid circulation in faults revealed by hematite (U-Th)/He and apatite fission-track dating: An example from Gower Peninsula fault fissures, Wales

Alexis K. Ault[1], Max Frenzel[2], Peter W. Reiners[3], Nigel H. Woodcock[4], and Stuart N. Thomson[3]
[1]DEPARTMENT OF GEOLOGY, UTAH STATE UNIVERSITY, 4505 OLD MAIN HILL, LOGAN, UTAH 84322, USA
[2]HELMHOLTZ-ZENTRUM DRESDEN-ROSSENDORF, HELMHOLTZ INSTITUTE FREIBERG FOR RESOURCE TECHNOLOGY, HALSBRÜCKER STRASSE 34, 09599, FREIBERG, GERMANY
[3]DEPARTMENT OF GEOSCIENCES, UNIVERSITY OF ARIZONA, 1040 E. 4TH STREET, TUCSON, ARIZONA 85721, USA
[4]DEPARTMENT OF EARTH SCIENCES, UNIVERSITY OF CAMBRIDGE, DOWNING STREET, CAMBRIDGE CB2 3EQ, UK

ABSTRACT

Fault rock low-temperature thermochronometry can inform the timing, temperature, and significance of hydrothermal fluid circulation in fault systems. We demonstrate this with combined hematite (U-Th)/He (He) dating, and sandstone apatite fission-track (AFT) and apatite and zircon (U-Th)/He (He) thermochronometry from fault-related fissures on the Gower Peninsula, Wales. Hematite He dates from 141 ± 5.1 Ma to 120 ± 5.0 Ma overlap with a 131 ± 20 Ma sandstone infill AFT date. Individual zircon He dates are 402–260 Ma, reflecting source material erosion, and imply a maximum Late Permian infill depositional age. Burial history reconstruction reveals modern exposures were not buried sufficiently in the Triassic–Early Cretaceous to have caused reheating to temperatures necessary to reset the AFT or hematite He systems, and thus these dates cannot reflect cooling due to erosion alone. Hot fluids circulating through fissures in the Early Cretaceous reset the AFT system. Hematite was either also reset by fluids or precipitated from these fluids. Similar hematite He dates from fault-related mineralization in south Glamorgan (Wales) and Cumbria (England) imply concomitant regional hot groundwater flow along faults. In this example, hydrothermal fluid circulation, coeval with North Atlantic rifting, occurred in higher-permeability fissures and fault veins long after they initially formed, directly influencing local and regional geothermal gradients.

LITHOSPHERE; v. 8; no. 4; p. 379–385; GSA Data Repository Item 2016168 | Published online 25 May 2016 doi:10.1130/L522.1

INTRODUCTION

Fault zones localize fluid and heat transfer in the upper crust (Sibson, 1981; Byerlee, 1993; Caine et al., 1996). Fault-hosted fluid circulation results in geochemical, mineralogical, rheological, and permeability changes that impact fault system evolution through time (Evans and Chester, 1995; Sibson, 2001). Depending on fault geometry and the permeability contrast between fault zone and country rock, hydrothermal fluids issuing along faults may advect significant heat, thereby influencing local and regional geothermal gradients. Hydrothermal fluid temperatures range up to 400 °C (Wilkinson, 2001; Yardley, 2005; Barker et al., 2010), and fluids may circulate through these zones for 10^3–10^6 yr (Lewchuk and Symons, 1995; Hickey et al., 2014), with fluid flux possible over longer (>10^7 yr) time intervals. Alteration and mineralization from fluids provide a direct record of thermal, geochemical, and deformational processes.

The temperature sensitivity of the hematite, apatite, and zircon (U-Th)/He (He) and apatite fission-track (AFT) systems makes these thermochronometry tools well suited to resolve the thermal imprint of hot fluid circulation, by documenting either the time of mineral formation or thermal resetting from fluids. Hematite, a common precipitate in hydrothermal systems, typically exhibits polydomain He diffusion behavior, and the hematite He method is sensitive to temperatures of ~25–250 °C, depending on the grain size of individual crystals in the polycrystalline aggregate and cooling rate (Farley and Flowers, 2012; Evenson et al., 2014). Apatite and zircon He thermochronometry record cooling through ~30–90 °C and ~50–250 °C, respectively, depending on the accumulation of radiation damage in the crystal (Flowers et al., 2009; Gautheron et al., 2009; Guenthner et al., 2013). The AFT method provides information about thermal histories in the ~100–120 °C temperature range (Gleadow et al., 2002). AFT systematics have been used to document the hydrothermal aureole around sizeable ore deposits (Hickey et al., 2014) and basin fluid circulation (Steckler et al., 1993).

In this contribution, we integrate multiple low-temperature thermochronometric datasets to decipher the timing and temperature of hydrothermal fluids issuing through fault zones. We specifically target minerals precipitated and directly entrained in faults because they are prime candidates for thermal resetting by hot fluid circulation. We apply this approach to a case study involving hematite mineralization and detrital apatite and zircon from surface-derived sedimentary infill in fault-related fissure fills on the Gower Peninsula, south Wales (Fig. 1). This is an ideal locality to test this approach owing to the presence of multiple datable phases in the fault zones themselves and the independently constrained, long-term burial and erosion history. We present fissure-fill hematite He and detrital apatite He, zircon He, and AFT thermochronometry data and compare these results to the regional burial and unroofing history to interpret the significance of the thermochronometry data.

FAULT-CONTROLLED HEMATITE MINERALIZATION

Fissures on the Gower Peninsula, Wales, located on the northern margin of Bristol Channel Basin (Fig. 1), preserve evidence of faulting, hematite-calcite mineralization, sediment infill, and paleofluid flow. The structure, mineralogy, and fill paragenesis have been detailed by George (1940), Roberts (1979), Wright et al. (2009), and Frenzel and Woodcock (2014). Summarized

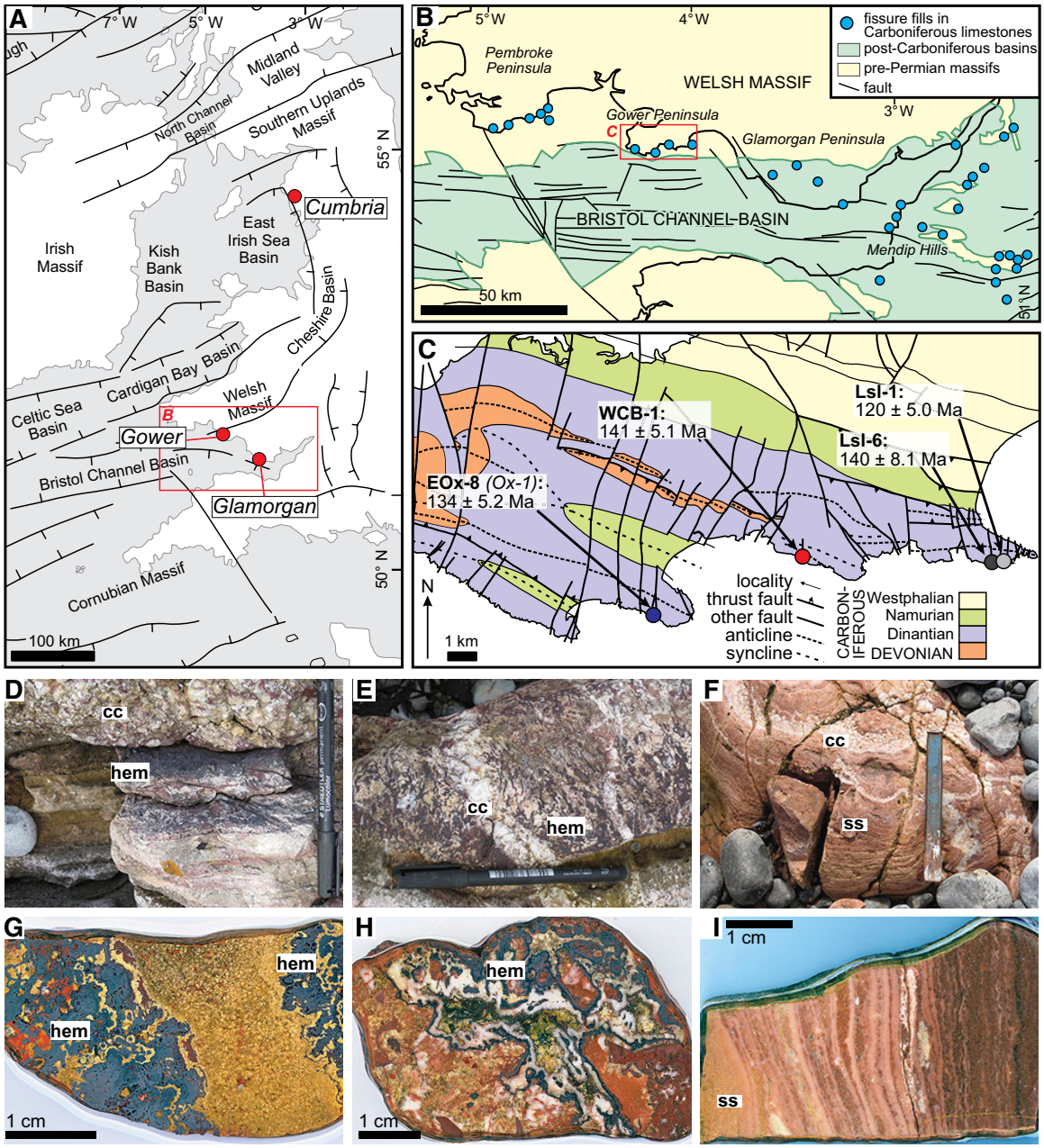

Figure 1. (A) Great Britain and Ireland location map highlighting massifs, basins, and the Gower, Glamorgan, and Cumbria locations. Box denotes location of B. (B) Simplified geologic map demarcating post-Carboniferous basins, and pre-Permian massifs, faults, and fissure fill localities around Bristol Channel Basin. Box denotes location of C. (C) Simplified geologic map of Gower peninsula showing the location of the four Gower hematite samples and sandstone sample, Ox-1. Hematite He dates are reported as mean ± 1σ standard deviation. (D–F) Field photographs of hematite (hem) and calcite (cc) fissure fill mineralization (D–E) and sandstone (ss) infill (F). (G–I) Corresponding polished sample chips highlight textures.

briefly here, hematite-calcite fissure-fills ~2–25 m wide are preserved in Devonian and Carboniferous rocks on the Gower Peninsula and occur along north-south–trending, subvertical, dilational, strike-slip fault zones (Fig. 1C). Fissures contain abundant void-filling calcite and botryoidal and specular hematite (Figs. 1D, 1E, 1G, and 1H), and lesser laminated sandy sediment with calcite cement and nanometer-thick hematite-coatings on individual quartz grains (Figs. 1F and 1I). Paragenetic sequences vary among Gower fissures, but they broadly exhibit common mineralization trends involving multiple early calcite generations and sedimentary infill, followed by hematite, ± dolomite, quartz, and ferroan calcite. Prior work demonstrated that the Gower fissures formed tectonically rather than by karst solution processes (Wright et al., 2009). Fault-hosted void spaces were filled and repeatedly brecciated, as evidenced by the crosscutting relationships of different mineralization events (Wright et al., 2009; Frenzel and Woodcock, 2014). The age and timescale(s) over which the Gower fissures formed and mineralization occurred are unknown. They have been variably attributed to late Carboniferous faulting (Wright et al., 2009) and Late Triassic rifting of the Bristol Channel Basin (Strahan, 1904; Woodcock et al., 2014).

Fault-controlled hematite vein mineralization developed elsewhere along the margin of the Bristol Channel Basin (Fig. 1B; Woodcock et al., 2014) and other Mesozoic basins in the UK, notably around the East Irish Sea Basin (Fig. 1A; Crowley et al., 2014). For comparison with the Gower data, we also targeted specular hematite from the Llanharry mine in the Vale of Glamorgan, ~20 km east of the Gower Peninsula (Figs. 1A and 1B), and botryoidal hematite from Cumbria, NW England (Fig. 1A). Mineralization at the Llanharry mine is confined to Carboniferous limestone capped by Triassic strata, and it is inferred to occur in the latest Triassic (Gayer and Criddle, 1970). Proposed Cumbrian ore deposit ages range from Carboniferous to Paleogene, and recent paleomagnetic data suggest a Middle Triassic age (Crowley et al., 2014).

HEMATITE SAMPLES AND TEXTURES

Four Gower samples (Lsl-1, Lsl-6, WCB-1, and EOx-8) were collected over a 15 km transect along the southern coast of the peninsula (Fig. 1C). Hematite exhibits macroscopic dendritic, botryoidal textures and is intimately associated with calcite, dolomite, and sandstone (Figs. 1D, 1E, 1G, and 1H; Fig. DR1[1]). Hematite and calcite are brecciated at the macroscale, but hematite crystals do not exhibit evidence for post-formation grain-size reduction or deformation.

Hematite aliquots were extracted from hand samples using tweezers and a portable rotary tool and were selected to avoid lobe exteriors and tool marks. Scanning electron microscopy (SEM) secondary electron (SE) imaging of representative aliquots revealed internal lobe texture and crystal morphology. Figure 2 presents representative SE images from select samples spanning the range of textures, and all images are catalogued in Figure DR2 (see footnote 1). SEM and crystal half-width measurement methods are detailed in the data repository item. Minimum and maximum crystal half-widths and corresponding closure temperatures (T_c), assuming hematite He diffusion kinetics and correspondence of observable crystal size and domain length scale as in Evenson et al. (2014), provide a first-order estimate of the temperature sensitivity of dated aliquots assuming a 10 °C/m.y. cooling rate (Table DR1).

Gower botryoidal hematite lobes exhibit intricate internal textures of densely packed platelets. Sample Lsl-1 consists of lobes of radially oriented plates. Locally, plates have a high aspect ratio and fan-like morphology, but elsewhere they are stacked, equant discs (Figs. 2A–2C). Plate half-widths are 75–175 nm, corresponding to apparent T_c of ~82–94 °C. Sample Lsl-6 similarly consists of variably and radially oriented plates (Fig. DR2). Plate half-widths are 50–200 nm, corresponding to $T_c \approx$ 77–96 °C. Sample EOx8 is composed of ≤20 µm botryoidal lobes with sublobes of parallel and radiating plates and high-aspect-ratio blades (Figs. 2D–2F). Uniform 30–40 nm plate half-widths correspond to $T_c \approx$ 70–74 °C. Sample WCB1 is a hybrid of Lsl-6 and EOX-8 textures, with alternating domains of lobes of thin, high-aspect-ratio blades and stacked, equant plates (Fig. DR2). Individual crystal half-widths of both morphologies are 25–50 nm, corresponding to $T_c \approx$ 68–77 °C. In contrast, Glamorgan sample LLW2 consists of macroscopically specular hematite (Figs. 2G–2I). Comparatively coarser-grained radial plates have variable half-widths of 0.5–5 µm and associated $T_c \approx$ 110–150 °C. Cumbria sample A14–11 exhibits macroscopic botryoidal texture with lobes up to 1 cm in diameter. Imaged and dated aliquots from a single sublayer have densely packed, high-aspect-ratio blades (Figs. 2J–2L). Crystal half-widths between 30 and 40 nm correspond to $T_c \approx$ 70–74 °C.

HEMATITE AND SEDIMENT INFILL THERMOCHRONOLOGY

We report hematite He data for 26 aliquots (Fig. DR3) from four Gower samples and individual samples from Glamorgan and Cumbria. Results are presented in Table DR2 and Figure 3A, and methods are detailed in the data repository item. Gower hematite He dates range from 140 ± 8.1 Ma to 120 ± 5.1 Ma, and dates were not all the same among fissures. Glamorgan sample LLW-2 yields a date of 97 ± 9.8 Ma (mean ± 1σ standard deviation of the mean), and Cumbria sample A14–11 yields a date of 117.4 ± 1.0 Ma. Most Gower and Cumbria dates show high intrasample reproducibility, with replicate aliquots overlapping within 2σ standard deviation. Three Gower samples yield a mean square of weighted deviates (MSWD) of 2.9–6.2 (Table DR2).

Apatite He, AFT, and zircon He data are from a sandstone infill sample (Ox-1; Figs. 1C, 1F, and 1I) taken from a fissure ~40 m from East Oxwich fissure hematite sample EOx-8, which exhibited dominantly calcite mineralization. Complementary hematite mineralization was not found in outcrop, but is likely present in inaccessible parts of the fissure. Limestone host rock did not yield apatite or zircon suitable for comparative thermochronology analyses. Poor Ox-1 apatite yield prevented measurement of a meaningful track length distribution. Results are reported in Tables DR3 and DR4 and Figure 3B. Details of analytical methods are provided in the data repository item. The apatite He date from this sample is 50.3 ± 7.3 Ma (n = 7), excluding one outlier at ca. 180 Ma, and the corresponding AFT date is 131 ± 20.1 Ma (central age ± 1σ). Individual zircon He dates are ca. 402–260 Ma, with a mean sample date of 308 ± 42.9 Ma (n = 8). There is no correlation between apatite He or zircon He date and effective U concentration (eU; calculated as [U] + 0.235 × [Th]; Fig. 3B) or grain size (Fig. DR4).

DISCUSSION

Regional Burial History of the Gower Peninsula

To evaluate the significance of the Gower hematite and sediment infill thermochronometry results, we first reconstruct the burial and erosion history of the Gower and Glamorgan Peninsulas from independent geologic constraints and plot this history in Figure 4A.

[1]GSA Data Repository Item 2016168, analytical methods for SEM, hematite He, apatite He, and AFT analyses, Tables DR1–DR4 (analytical results), Figure DR1 (hand sample photographs), Figure DR2 (SEM image catalogue), Figure DR3 (dated hematite aliquot photographs), Figure DR4 (apatite and zircon He data), and Figure DR5 (hematite He data), is available at www.geosociety.org/pubs/ft2016.htm, or on request from editing@geosociety.org.

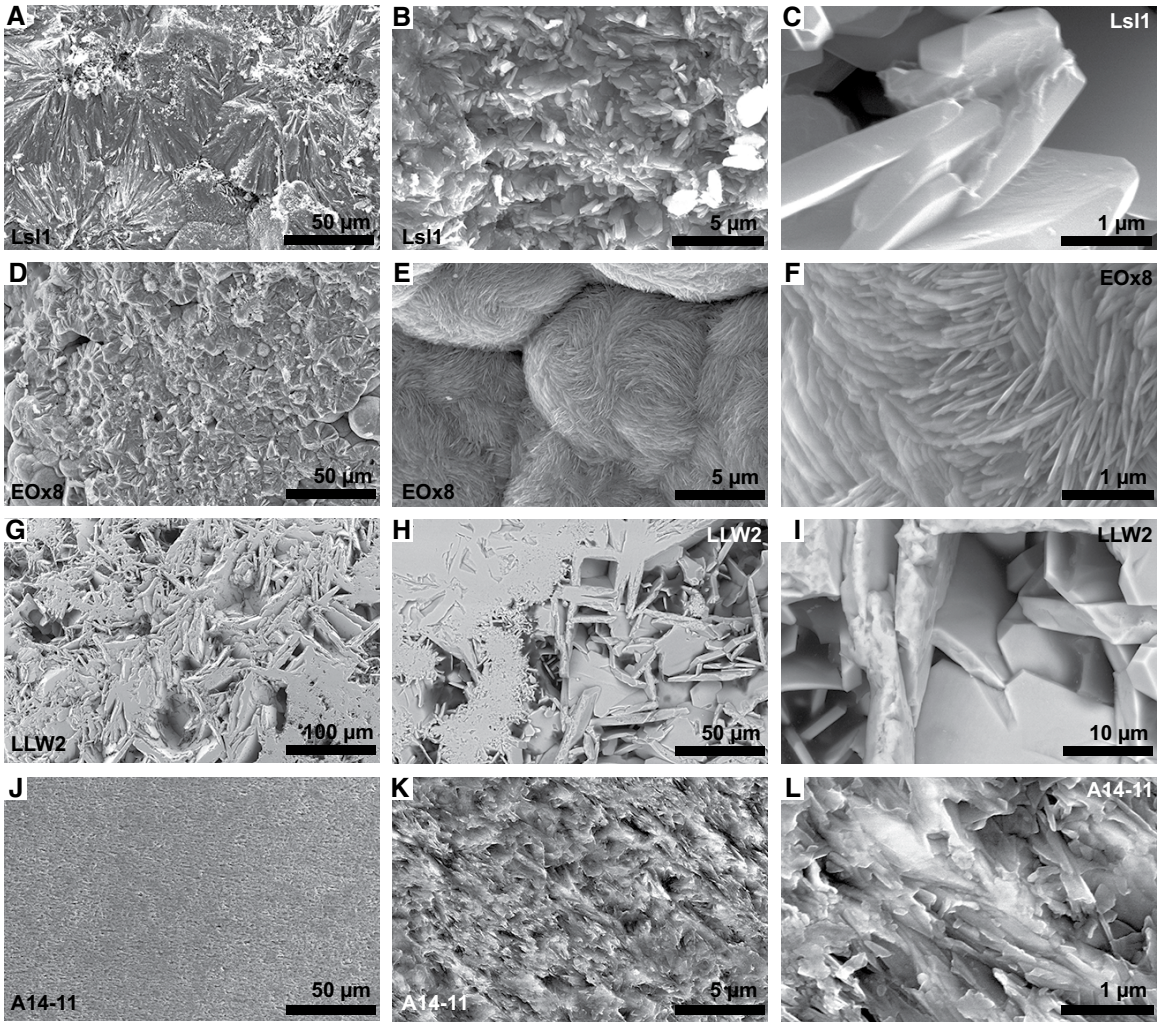

Figure 2. Scanning electron microscopy (SEM) secondary electron (SE) images of representative hematite aliquots at three different scales from Gower samples Lsl-1 (A–C) and EOx-8 (D–F), Glamorgan sample LLW-2 (G–I), and Cumbria sample A14–11 (K–L).

Early Carboniferous limestone hosting the fissures was buried beneath the south Wales coal basin, preserved north of Gower, to depths of ~3 km during the mid- to late Carboniferous (Burgess and Gayer, 2000). Folding and thrusting associated with the Variscan orogeny in the late Carboniferous–Early Permian likely resulted in ≤2× tectonic thickening, and the structural thickness above the Carboniferous limestone may have reached ~4.5 km (Burgess and Gayer, 2000). Post-Carboniferous cover was subsequently eroded away, as constrained by an Early Triassic unconformity directly overlying the Llanharry hematite deposits in Glamorgan and a Triassic outlier near the Gower Oxwich sample localities (George, 1940). Norian (ca. 228–204 Ma) fossils in multiple fissures around the Bristol Channel Basin imply fissures were at the surface at that time (Benton and Spencer, 1995; Whiteside and Marshall, 2008). Subsequent Bristol Channel Basin (Figs. 1A and 1B) subsidence south of Gower and Glamorgan resulted in deposition of a few hundred meters, and no more than a kilometer, of Triassic and Jurassic strata in the center of the basin (Lloyd et al., 1973; Van Hoorn, 1987). In the Early Cretaceous, regional extension, including faulting on the Bristol Channel fault, caused erosion of the northern footwall and subsidence of the southern hanging wall (Van Hoorn, 1987). A Late Cretaceous marine transgression from postrifting thermal subsidence and eustasy deposited ≤1 km of chalk in the center of the Bristol Channel Basin, with less on Gower and Glamorgan along the northern basin margin (Van Hoorn, 1987). Latest Cretaceous–Paleogene unroofing reflects combined effects of sea-level fall and marine regression (Miller et al., 2005), possible crustal compression and associated exhumation (Hillis et al., 2008), peripheral Thulean volcanism, and the onset of thermal uplift linked to the Icelandic plume across NW Britain (Nadin et al., 1997; Clift et al., 1998). In summary, the deepest burial of the Gower fissures and limestone host rocks occurred ca. 290 Ma. Present-day exposures were exhumed to the near surface by the Late Triassic and have remained there (or at depths significantly <1 km; Fig. 4A).

Detrital Zircon (U-Th)/He Constraints on Gower Burial History

Zircon He dates from sandstone infill range from ca. 402 to 260 Ma (Fig. 3B). The absence of date-eU (Fig. 3B) and date–grain size (Fig. DR4) correlations suggests zircons did not experience partial He loss from protracted elevated

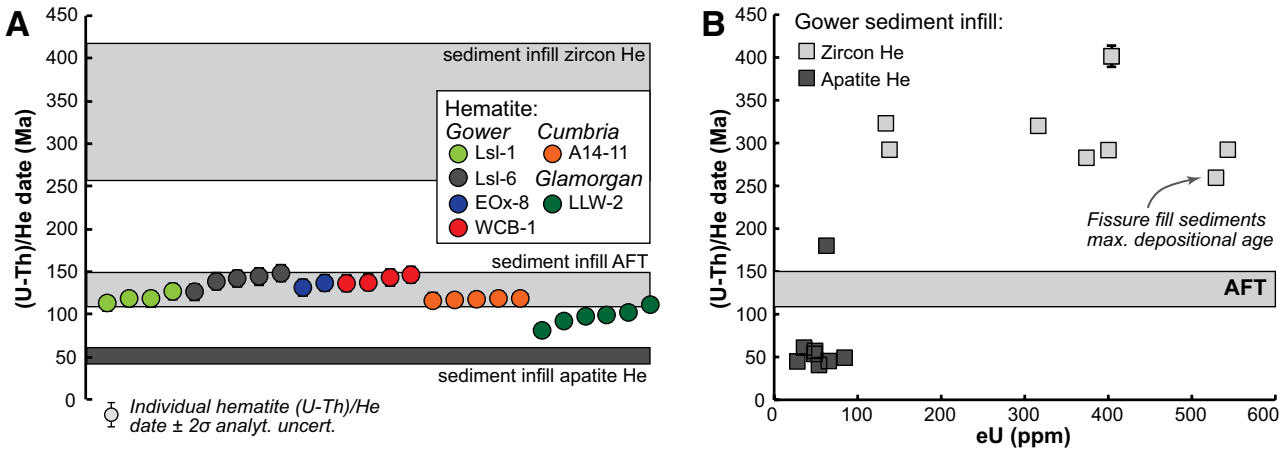

Figure 3. (A) Individual hematite (U-Th)/He (He) dates plotted with 2σ analytical uncertainties and classified by sample. Ranges of zircon He, apatite fission-track (AFT), and apatite He dates shown for reference. (B) Individual zircon and apatite (U-Th)/He dates as a function of eU for sample Ox-1. Central AFT date ± 1σ standard deviation is illustrated with gray bar.

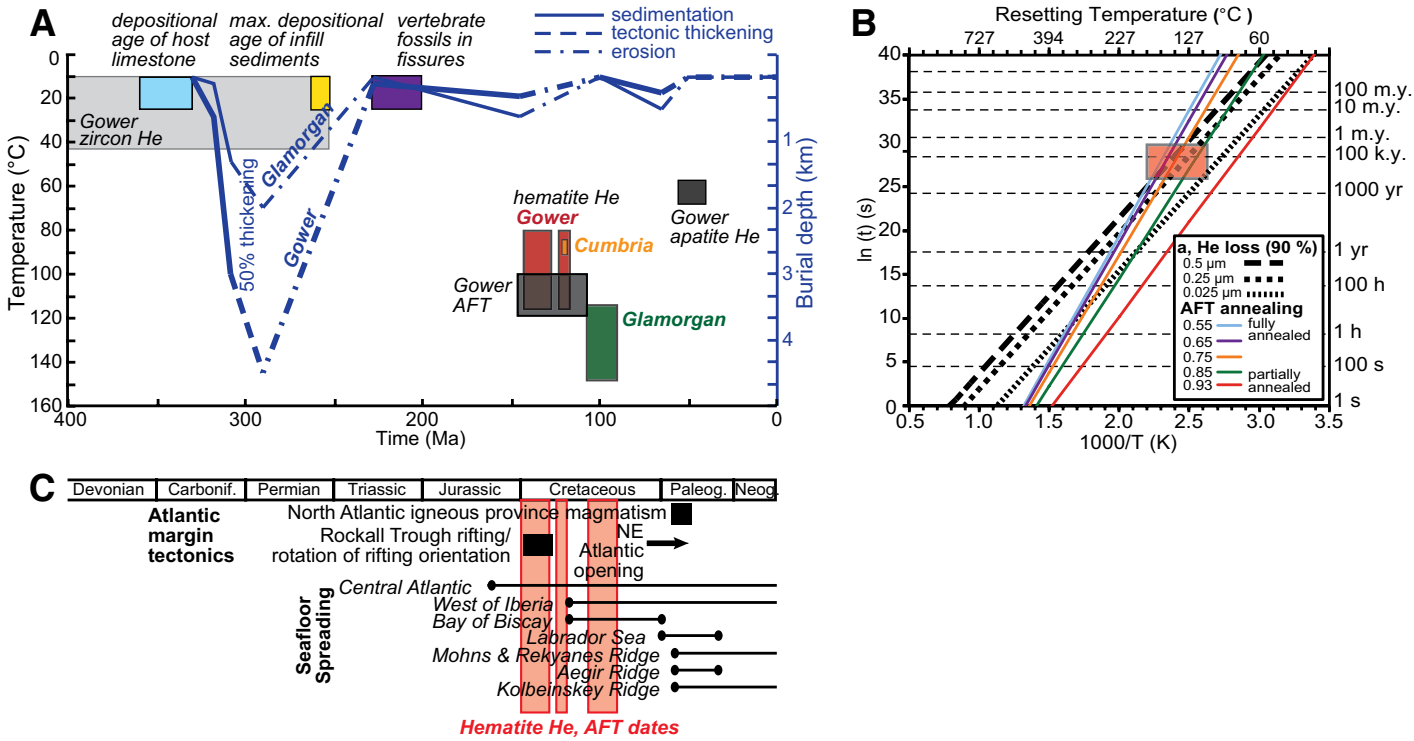

Figure 4. (A) Burial history curve for Gower and Glamorgan over the last ~400 m.y. (blue curves, right *y*-axis). Temperatures estimated assuming 30 °C/km geotherm and 10 °C surface temperature. Legend for process (e.g., sedimentation, tectonic thickening, erosion) given in upper right. Bold line—Gower; thin line—Glamorgan. Hematite (U-Th)/He (He) and Gower sedimentary infill zircon He, apatite fission-track (AFT), and apatite He data are plotted as a function of temperature sensitivity (left *y*-axis) and date. (B) Temperature and time required to reset the hematite He and AFT systems. Hematite He 90% fractional loss contours as a function of time and the inverse of temperature calculated from a square pulse-heating event. Calculations use an activation energy of 147.5 kJ/mol and D_0 of 2.2E–04 cm²/s (Evenson et al., 2014) and 0.5, 0.25, and 0.025 μm diffusion domain length scales encompassing the majority of plate thicknesses from backscattered electron (BSE) images. Complementary AFT track annealing calculations are given for *r* values (= reduced length normalized to unannealed length) of 0.55 (fully annealed) to 0.93 (not annealed). Red polygon highlights temperature and duration of heating required to reset both the hematite He and AFT systems. (C) Timing of major North Atlantic tectonic and seafloor spreading events with hematite He date ranges highlighted in red; same time (*x*-axis) as in A; modified from Holford et al. (2005).

temperatures associated with reburial. We interpret these data to record cooling and erosion of the source material derived from the Variscan orogen to the south. Zircons were transported and deposited in the fissures after ca. 260 Ma, and were not reset by reheating, consistent with the aforementioned burial history (Fig. 4A). The youngest zircon He date thus broadly reflects a maximum depositional age for sandstone within the fissures. Sediments may have been incorporated into fissures during the Late Triassic, consistent with vertebrate fossil evidence (Fig. 4A; Benton and Spencer, 1995; Whiteside and Marshall, 2008). This does not preclude initial faulting and fissure formation prior to ca. 260 Ma or Late Triassic time, nor does it imply that the sandstone infill event and hematite precipitation were necessarily coeval.

Hematite (U-Th)/He and AFT Dates Record Paleofluid Flow in Gower Fissures

We interpret concordant hematite He and AFT dates from fault material within the Gower fissures to reflect thermal resetting from hot fluid circulation through these higher-permeability fault zones. Comparison between these data and the reconstructed Gower burial history indicates dates cannot simply record cooling due to erosional exhumation (Fig. 4A). Estimated Gower hematite He T_c values of ~80–115 °C (Table DR1) overlap the nominal AFT T_c. Gower fissures were likely at near-surface conditions in the Triassic, and subsequent Jurassic–earliest Cretaceous burial of modern south Wales exposures did not exceed several hundred meters (Fig. 4A). For Early Cretaceous hematite He and AFT dates to reflect postburial regional cooling from erosion requires an untenable ambient geothermal gradient of ~265–400 °C/km, assuming 300 m of cover.

Two potential scenarios explain the fissure-fill hematite He and AFT dates. First, hematite precipitated in the Late Triassic or possibly Carboniferous. Hot fluids circulating through these higher-permeability fissures in the Early Cretaceous reset both hematite He and AFT systems with similar temperature sensitivity. Alternatively, hematite formed in the Early Cretaceous, and localized but widely distributed hot fluids associated with this mineralization event induced infill AFT resetting. At present, it is not possible to discriminate between these two possibilities. In either case, these data imply that the higher-permeability fissures served as conduits for hydrothermal fluid circulation long after their formation.

Gower hematite He and sedimentary infill AFT dates are consistent with some published AFT data from northern England and the margins of the central Irish Sea Basin (Fig. 1A; Duncan et al., 1998; Green et al., 2001; Holford et al., 2005). We acknowledge heterogeneity in the magnitude of pre–Early Cretaceous regional burial and the impact of likely thicker sedimentary cover in and around the Irish Sea Basin on AFT dates. However, we note regional low-temperature thermochronology–derived thermal histories may reflect fluid-mediated heat transfer along faults and associated elevated geothermal gradient in addition to the effects of subsidence and sedimentation. For example, variable Cenozoic low-temperature thermochronometry–based exhumation estimates from the British Isles and Irish Sea Basin region (e.g., Hillis et al., 2008) may track variations in geothermal gradient in space and time.

Early Cretaceous hot fluids would have similarly reset the lower T_c apatite He system at that time. The ca. 50 Ma sandstone infill apatite He date reflects subsequent He loss from reheating due to reburial beneath Late Cretaceous chalk. Late Paleocene igneous activity may have elevated the regional geothermal gradient (~60 °C/km) at that time. However, chalk has low thermal conductivity (<2.0 W/mK) compared to limestone (2.0–3.4 W/mK) and thus likely acted as a thermal blanket, resulting in an increased near-surface geothermal gradient for a given basal heat flow. In either case, our apatite He data are consistent with reported ~1.4–1.0 km of Paleocene–Eocene exhumation ~75 km north of Gower Peninsula (Hillis et al., 2008).

Hematite He, AFT, and zircon He systematics constrain minimum Late Cretaceous fluid temperatures. The calculated fluid temperature and heat duration required to reset the hematite He and AFT systems (He loss and fission-track annealing, respectively) are ~100–150 °C for 10^5–10^6 yr (Fig. 4B), consistent with estimates for fluid circulation in fault zones (Lewchuk and Symons, 1995; Hickey et al., 2014). Zircon He data patterns also suggest fluid temperatures did not exceed ~180–200 °C. Hematite He dates from fault-related hematite mineralization in Glamorgan and Cumbria overlap with the Gower results and suggest that similar Late Cretaceous hot fluids operated regionally. We interpret the slightly younger mean Glamorgan hematite He date (Fig. 3A), in spite of larger mean crystal size, to reflect combined effects of hotter fault-hosted temperatures near the center of the Bristol Channel Basin or later hematite formation.

Implications of Fault-Hosted Fluid Circulation in Ancient Fault Zones

Local fluid flux and advection of heat in fault zones and fracture networks may result in mineralization and/or thermal resetting of not only fault rocks themselves, but also the surrounding host rock. This has direct implications for local and regional upper-crustal geothermal gradient estimates. Our results show that higher-permeability faults, fissures, and fault veins can serve as conduits for fluid and heat transfer, even long after these structures initially formed. Thus, increases in geothermal gradient in ancient fault zones may be decoupled from initial tectonism and fault formation. Long-term effects on local and regional geotherms should be taken into consideration when reconstructing burial and exhumation estimates from low-temperature thermochronometry–derived thermal histories. In our Gower example, we document Early Cretaceous hydrothermal fluid circulation in originally Variscan fault zones. Fluid circulation in Gower fissures was coeval with tectonic and seafloor spreading events associated with the opening of the North Atlantic Ocean (Fig. 4C; Dore et al., 1999). We suggest that low-temperature thermochronometry of targeted fault materials can constrain the timing and thermal signatures of localized fault-hosted paleofluid flows that may be a manifestation of regional, or even global, plate-tectonic processes.

ACKNOWLEDGMENTS

We thank Uttam Chowdhury and Fen-Ann Shen for analytical assistance. We thank Ben van der Pluijm, an anonymous reviewer, and Editor Arlo Weil for constructive reviews that improved the manuscript. We acknowledge support from the National Science Foundation through grants EAR-1419828 to Ault and Reiners and EAR-1219653 to Reiners, and from the Utah State University Microscopy Core Facility.

REFERENCES CITED

Barker, A.K., Coogan, L.A., Gillis, K.M., Hayman, N.W., and Weis, D., 2010, Direct observation of a fossil high-temperature, fault-hosted, hydrothermal upflow zone in crust formed at the East Pacific Rise: Geology, v. 38, p. 379–382, doi:10.1130/G30542.1.

Benton, M., and Spencer, P.S., 1995, Fossil Reptiles of Great Britain: Geological Conservation Review Series 10: Peterborough, UK, Joint Nature Conservation Committee, 386 p.

Burgess, P.M., and Gayer, R.A., 2000, Late Carboniferous tectonic subsidence in south Wales: Implications for Variscan basin evolution and tectonic history in SW Britain: Journal of the Geological Society, London, v. 157, p. 93–104, doi:10.1144/jgs.157.1.93.

Byerlee, J., 1993, Model for episodic flow of high-pressure water in fault zones before earthquakes: Geology, v. 21, p. 303–306, doi:10.1130/0091-7613(1993)021<0303:MFEFOH>2.3.CO;2.

Caine, J.S., Evans, J.P., and Forster, C.B., 1996, Fault zone architecture and permeability structure: Geology, v. 24, p. 1025–1028, doi:10.1130/0091-7613(1996)024<1025:FZAAPS>2.3.CO;2.

Clift, P.D., Carter, A., and Hurford, A.J., 1998, The erosional and uplift history of NE Atlantic passive margins: Constraints on a passing plume: Journal of the Geological Society, London, v. 155, p. 787–800, doi:10.1144/gsjgs.155.5.0787.

Crowley, S.F., Piper, J.D.A., Bamarouf, T., and Roberts, A.P., 2014, Paleomagnetic evidence for the age of the Cumbrian and Manx hematite ore deposits: Implications for the origin of hematite mineralization at the margins of the East Irish Sea Basin, UK: Journal of the Geological Society, London, v. 171, p. 49–64, doi:10.1144/jgs2013-004.

Dore, A.G., Lundin, E.R., Jensen, L.N., Birkeland, O., Eliassen, P.E., and Fichler, C., 1999, Principal tectonic events in the

evolution of the northwest European Atlantic margin, *in* Fleet, A.J., and Boldy, S.A.R., eds., Petroleum Geology of Northwest Europe: Proceedings of the 5th Conference: London, Geological Society, p. 41–61.

Duncan, W.I., Green, P.F., and Duddy, I.R., 1998, Source rock burial history and seal effectiveness: Key facets to understanding hydrocarbon exploration potential in the East and Central Irish Sea Basins: American Association of Petroleum Geologists Bulletin, v. 82, p. 1401–1415.

Evans, J.P., and Chester, F.M., 1995, Fluid-rock interaction in faults of the San Andreas system: Inferences from San Gabriel fault rock geochemistry and microstructures: Journal of Geophysical Research, v. 100, p. 13,007–13,020, doi:10.1029/94JB02625.

Evenson, N.S., Reiners, P.W., Spencer, J., and Shuster, D.L., 2014, Hematite and Mn oxide (U-Th)/He dates from the Buckskin-Rawhide detachment system, western Arizona: Constraining the timing of mineralization and hematite (U-Th)/He systematics: American Journal of Science, v. 314, p. 1373–1435, doi:10.2475/10.2014.01.

Farley, K.A., and Flowers, R.M., 2012, (U-Th)/Ne and multidomain (U-Th)/He systematics of a hydrothermal hematite from eastern Grand Canyon: Earth and Planetary Science Letters, v. 359–360, p. 131–140, doi:10.1016/j.epsl.2012.10.010.

Flowers, R.M., Ketcham, R.A., Shuster, D.L., and Farley, K.A., 2009, Apatite (U-Th)/He thermochronometry using a radiation damage accumulation and annealing model: Geochimica et Cosmochimica Acta, v. 73, p. 2347–2365, doi:10.1016/j.gca.2009.01.015.

Frenzel, M., and Woodcock, N.H., 2014, Cockade breccia: Product of mineralisation along dilational faults: Journal of Structural Geology, v. 68, p. 194–206, doi:10.1016/j.jsg.2014.09.001.

Gautheron, C., Tassan-Got, L., Barbarand, J., and Pagel, M., 2009, Effect of alpha-damage annealing on apatite (U-Th)/He thermochronology: Chemical Geology, v. 266, p. 157–170, doi:10.1016/j.chemgeo.2009.06.001.

Gayer, R.A., and Criddle, A.J., 1970, Mineralogy and genesis of Llanharry iron ore deposits, Glamorgan, *in* Mining and Petroleum Geology, Proceedings of the Ninth Commonwealth Mining and Metallurgical Congress 1969, Volume 2: London, Institution of Mining and Metallurgy, p. 605–626.

George, T.N., 1940, The structure of Gower: Quarterly Journal of the Geological Society, London, v. 96, p. 131–198, doi:10.1144/GSL.JGS.1940.096.01-04.06.

Gleadow, A.J.W., Belton, D.X., Kohn, B.P., and Brown, R.W., 2002, Fission track dating of phosphate minerals and the thermochronology of apatite: Reviews in Mineralogy and Geochemistry, v. 48, p. 579–630, doi:10.2138/rmg.2002.48.16.

Green, P.F., Duddy, I.R., Bray, R.J., Duncan, W.I., and Corcoran, D.V., 2001, The influence of thermal history on hydrocarbon prospectivity in the Central Irish Sea Basin, *in* Shannon, P.M., Haughton, P.D.W., and Corcoran, D.V., eds., The Petroleum Exploration of Ireland's Offshore Basins: Geological Society, London, Special Publication 188, p. 171–188.

Guenthner, W.R., Reiners, P.W., Ketcham, R.A., Nasdala, L., and Giester, G., 2013, Helium diffusion in natural zircon: Radiation damage, anisotropy, and the interpretation of zircon (U-Th)/He thermochronology: American Journal of Science, v. 313, p. 145–198, doi:10.2475/03.2013.01.

Hickey, K.A., Barker, S.L.L., Dipple, G.M., Arehart, G.B., and Donelick, R.A., 2014, The brevity of hydrothermal fluid flow revealed by thermal halos around giant gold deposits: Implications for Carlin-type gold systems: Economic Geology and the Bulletin of the Society of Economic Geologists, v. 109, p. 1461–1487, doi:10.2113/econgeo.109.5.1461.

Hillis, R.R., Holford, S.P., Green, P.F., Dore, A.G., Gatliff, R.W., Stoker, M.S., Thomson, K., Turner, J.P., Underhill, J.R., and Williams, G.A., 2008, Cenozoic exhumation of the southern British Isles: Geology, v. 36, p. 371–374, doi:10.1130/G24699A.1.

Holford, S.P., Turner, J.P., and Green, P.F., 2005, Reconstructing the Mesozoic–Cenozoic exhumation history of the Irish Sea Basin system using apatite fission track analysis and vitrinite reflectance data, *in* Dore, A.G., and Vinning, B.A., eds., Petroleum Geology: North-West Europe and Global Perspectives—Proceedings of the 6th Petroleum Geology Conference: London, Geological Society, p. 1095–1107.

Lewchuk, M.T., and Symons, D.T.A., 1995, Age and duration of Mississippi Valley–type ore-mineralizing events: Geology, v. 23, p. 233–236, doi:10.1130/0091-7613(1995)023<0233:AADOMV>2.3.CO;2.

Lloyd, A.J., Savage, R.J.G., Stride, A.H., and Donovan, D.T., 1973, The geology of the Bristol Channel floor: Philosophical Transactions of the Royal Society of London, v. 274, p. 595–626, doi:10.1098/rsta.1973.0077.

Miller, K.G., Kominz, M.A., Browning, J.V., Wright, J.D., Mountain, G.S., Katz, M.E., Sugarman, P.J., Cramer, B.S., Christie-Blick, N., and Pekar, S.F., 2005, The Phanerozoic record of global sea-level change: Science, v. 310, p. 1293–1298, doi:10.1126/science.1116412.

Nadin, P.A., Kusznir, N.J., and Cheadle, M.J., 1997, Early Tertiary plume uplift of the North Sea and Faeroe-Shetland Basins: Earth and Planetary Science Letters, v. 148, p. 109–127, doi:10.1016/S0012-821X(97)00035-6.

Roberts, J.C., 1979, Jointing and minor tectonics of the south Gower Peninsula between Mumbles Head and Rhossili Bay, south Wales: Geological Journal, v. 14, p. 1–14.

Sibson, R.H., 1981, Fluid flow accompanying faulting: Field evidence and models, *in* Simpson, D.W., and Richards, P.G., eds., Earthquake Prediction—An International Review: American Geophysical Union Maurice Ewing Monograph 4, p. 593–603.

Sibson, R.H., 2001, Seismogenic framework for hydrothermal transport and ore deposition: Reviews in Economic Geology, v. 14, p. 25–50.

Steckler, M.S., Omar, G.I., Karner, G.D., and Kohn, B.P., 1993, Pattern of hydrothermal circulation within the Newark Basin from fission-track analysis: Geology, v. 21, p. 735–738, doi:10.1130/0091-7613(1993)021<0735:POHCWT>2.3.CO;2.

Strahan, A, and Cantrill, T.C., 1904, The geology of the South Wales coalfield: Part VI., in Memoirs of the Geological Survey of England and Wales, Order of the Lords Commissioners of His Majesty's Treasury, 120 p.

Van Hoorn, B., 1987, The south Celtic Sea–Bristol Channel Basin: Origin, deformation, and inversion history: Tectonophysics, v. 137, p. 309–334, doi:10.1016/0040-1951(87)90325-8.

Whiteside, D.I., and Marshall, J.E.A., 2008, The age, fauna, and paleoenvironment of the Late Triassic fissure deposits of Tytherington, South Gloucestershire, UK: Geological Magazine, v. 145, p. 105–147, doi:10.1017/S0016756807003925.

Wilkinson, J.J., 2001, Fluid inclusions in hydrothermal ore deposits: Lithos, v. 55, p. 229–272, doi:10.1016/S0024-4937(00)00047-5.

Woodcock, N.H., Miller, A.V.M., and Woodhouse, J.H., 2014, Chaotic breccia zones on the Pembroke Peninsula, south Wales: Evidence for collapse into voids along dilational faults: Journal of Structural Geology, v. 69, p. 91–107, doi:10.1016/j.jsg.2014.09.019.

Wright, V., Woodcock, N.H., and Dickson, J.A.D., 2009, Fissure fills along faults: Variscan examples from Gower, south Wales: Geological Magazine, v. 146, p. 890–902, doi:10.1017/S001675680999001X.

Yardley, B.W.D., 2005, Metal concentrations in crustal fluids and their relationship to ore formation: Economic Geology and the Bulletin of the Society of Economic Geologists, v. 1000, p. 613–632.

MANUSCRIPT RECEIVED 3 FEBRUARY 2016
REVISED MANUSCRIPT RECEIVED 24 APRIL 2016
MANUSCRIPT ACCEPTED 12 MAY 2016

Printed in the USA